AD-A071 444 NAVAL RESEARCH LAB WASHINGTON DC F/G 17/1
HYDROPHONE PHASE STABILITY ANALYSIS AT FREQUENCIES BELOW 100 HZ--ETC(U)
JUL 79 A C TIMS, T A HENRIQUEZ

UNCLASSIFIED NRL-8314 NL

| OF |
AD
A071444

END
DATE
FILMED
9-79
DDC

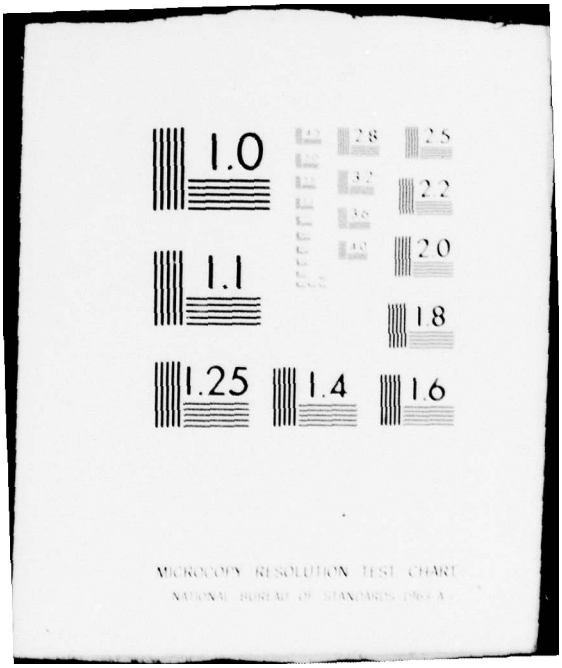
1.0
1.1
1.25
1.4
1.6
2.8
3.2
3.6
4.0
2.5
2.2
2.0
1.8
MICROCOPY RESOLUTION TEST CHART
NATIONAL BUREAU OF STANDARDS 1963-A

NRL Report 8314

Hydrophone Phase Stability Analysis at Frequencies Below 100 Hz

A. C. Tims and T. A. Henriquez

Transducer Branch
Underwater Sound Reference Detachment
P. O. Box 8337
Orlando, Florida 32856

LEVEL II

July 9, 1979

NAVAL RESEARCH LABORATORY
Washington, D.C.

SECURITY CLASSIFICATION OF THIS PAGE (When Data Entered)

REPORT DOCUMENTATION PAGE

READ INSTRUCTIONS BEFORE COMPLETING FORM

1. REPORT NUMBER: NRL Report 8314
2. GOVT ACCESSION NO.
3. RECIPIENT'S CATALOG NUMBER

4. TITLE (and Subtitle): HYDROPHONE PHASE STABILITY ANALYSIS AT FREQUENCIES BELOW 100 Hz
5. TYPE OF REPORT & PERIOD COVERED: Interim report on one phase of a continuing NRL problem
6. PERFORMING ORG. REPORT NUMBER

7. AUTHOR(s): A.C. Tims and T.A. Henriquez
8. CONTRACT OR GRANT NUMBER(s): F11101

9. PERFORMING ORGANIZATION NAME AND ADDRESS
Underwater Sound Reference Detachment
Naval Research Laboratory
P.O. Box 8337, Orlando, FL 32856

10. PROGRAM ELEMENT, PROJECT, TASK AREA & WORK UNIT NUMBERS
NRL Problem S02-51
Program Element 62711N-11
Project ZF11 121 003

11. CONTROLLING OFFICE NAME AND ADDRESS
Underwater Sound Reference Detachment
Naval Research Laboratory
P.O. Box 8337, Orlando, FL 32856

12. REPORT DATE: July 1979
13. NUMBER OF PAGES: 23

14. MONITORING AGENCY NAME & ADDRESS (if different from Controlling Office)
12 24p.

15. SECURITY CLASS. (of this report): UNCLASSIFIED
15a. DECLASSIFICATION/DOWNGRADING SCHEDULE

16. DISTRIBUTION STATEMENT (of this Report)

Approved for public release; distribution unlimited.

14 NRL-8314

17. DISTRIBUTION STATEMENT (of the abstract entered in Block 20, if different from Report)

18. SUPPLEMENTARY NOTES

19. KEY WORDS (Continue on reverse side if necessary and identify by block number)

Hydrophone	Preamplifier
Low frequency	Pressure stability
Phase analysis	Temperature stability

20. ABSTRACT (Continue on reverse side if necessary and identify by block number)

The design criterion for a standard reference hydrophone for accurate phase measurements independent of temperature and hydrostatic pressure is examined. Geometrical, acoustical, and electrical considerations that determine the electroacoustic phase response of a hydrophone are analyzed to optimize phase stability within specific frequency ranges. Limitations due to pyroelectric effect and low-frequency piezoelectric response are analyzed and specific examples given.

251 950

DD FORM 1 JAN 73 1473 EDITION OF 1 NOV 65 IS OBSOLETE
S/N 0102-014-6601

SECURITY CLASSIFICATION OF THIS PAGE (When Data Entered)

79 07 19 007

CONTENTS

HYDROPHONE PHASE STABILITY ANALYSIS AT FREQUENCIES BELOW 100 Hz

INTRODUCTION

For many years, the Underwater Sound Reference Detachment (USRD) has provided a variety of broadband environmentally stable transducers and hydrophones for use by the underwater acoustic community. The mission and program of the USRD have consistently focused on the development of new or improved underwater acoustic standards, which is determined primarily by user needs or the advancing state-of-the-art.

In more recent years, increased efforts in the detection of acoustical energy by passive sonar signal processing have emphasized the need for high-resolution phase measurements. The Navy depends on measurements of electrical phase between acoustic sensors for surveillance systems, sound propagation information, antisubmarine warfare, and oceanographic efforts. To effectively determine the phase characteristics of an unknown hydrophone requires a reference standard with well-defined phase characteristics. The reference standard should have a phase response that is constant with frequency and environmentally stable.

PURPOSE

The purpose of this investigation was to identify the problems associated with acoustic calibration measurements related to a change of phase in the electroacoustic instrumentation (especially in the hydrophone sensor and preamplifier, at infrasonic and low-audio frequencies). The intent was to implement a design criterion for a phase-stable piezoelectric reference standard hydrophone for use at infrasonic and low-audio frequencies, in the temperature range −2 to +40°C and at hydrostatic pressures to 70 MPa.

THE HYDROPHONE SENSOR-PREAMPLIFIER

Many of the problems associated with calibration measurements relating to the acoustic phase are inherent to the hydrophone sensor and preamplifier input impedance. Figure 1 shows a simplified diagram of a typical hydrophone circuit where C_s is the sensor capacitance, C_1 is the input coupling capacitor, R_2 is the calibration resistor, and R_1 is the fixed input impedance of amplifier $A1$. Given that $A1$ does not have an internal phase shift, C_1 is about two orders of magnitude greater than C_s, and the frequency is well below the fundamental electroacoustic resonance of the sensor, then the circuit components can be lumped into a simple RC circuit.

Manuscript submitted March 27, 1979.

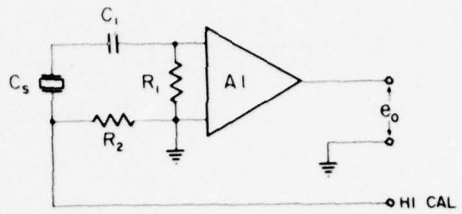

Fig. 1 — Simplified schematic of a typical hydrophone circuit

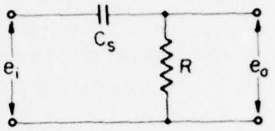

Fig. 2 — First-order high-pass filter

The sensor capacitance and the input resistance combined form a first-order high-pass filter, as shown in Fig. 2. The frequency-response function for sine-wave inputs is

$$F(\omega) = \frac{e_o}{e_i} = \frac{j\omega RC_s}{1 + j\omega RC_s}. \tag{1}$$

Equation (1) gives both gain and phase for the circuit. The gain or amplitude A is obtained by taking the square root of the sum of the squares of the real and imaginary parts:

$$A = \frac{e_o}{e_i} = \frac{1}{(1 + 1/\omega^2 R^2 C_s{}^2)^{1/2}}. \tag{2}$$

The break frequency or down frequency of -3 dB is given by

$$f_{-3\text{ dB}} \equiv f_o = \frac{1}{2\pi RC_s} \tag{3}$$

$$\Rightarrow RC_s = \frac{1}{\omega_o} \tag{4}$$

where $\omega_o = 2\pi f_o$. Substituting Eq. (4) in Eq. (2) leads to

$$A = \left(1 + \frac{\omega_o{}^2}{\omega^2}\right)^{-1/2} \text{ or } \left(1 + \frac{f_o{}^2}{f^2}\right)^{-1/2} \tag{5}$$

The low-frequency filter attenuation or low-frequency roll-off in decibels for any frequency f is

$$20 \log A = -10 \log \left(1 + \frac{f_o{}^2}{f^2}\right). \tag{6}$$

The tangent of the phase angle ϕ is given by the ratio of the imaginary and real parts of the filter impedance, which from Eq. (1) will give

$$\phi = \tan^{-1}\left(\frac{1}{\omega R C_s}\right). \tag{7}$$

If desired, Eq. (4) can be substituted in Eq. (7) yielding

$$\phi = \tan^{-1}\left(\frac{f_o}{f}\right). \tag{8}$$

A plot of the amplitude and phase as a function of frequency is shown in Fig. 3. The slope of the amplitude is 6 dB per octave or 20 dB per decade. The figure shows that the amplitude is not constant with frequency until the frequency is a decade above f_o and the phase is not constant until two decades above f_o. Therefore, if a hydrophone is to have a constant phase response down to some low frequency f, then the break frequency f_o would have to be set two decades below f.

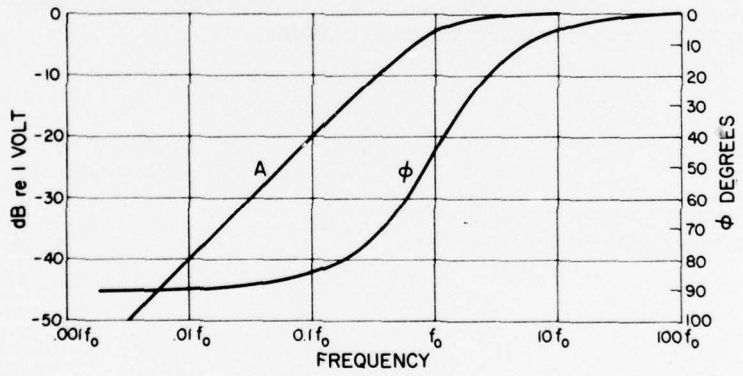

Fig. 3 — Amplitude (A) and phase angle (ϕ) of a first-order high-pass filter as a function of frequency

Only the first-order high-pass filter has been analyzed for the hydrophone input for several reasons. First, for a piezoelectric sensor hydrophone its use is virtually a physical inevitability. The sensor will always have some finite capacitance and the preamplifier some finite input impedance. Second, a first-order filter is easily implemented in very high impedance circuits and presents a minimum insertion loss. Finally, and most important for this investigation, it has a lower and smoother phase shift than higher order filter networks.

RADIATION LOAD EFFECTS

The sensor is analogous to a sphere, regardless of its specific configuration for purposes of phase analysis in the infrasonic and low-audio frequency ranges where the dimensions of

a hydrophone sensor are very small compared to the acoustic wavelength. The lumped-parameter equivalent circuit for a thin-walled ceramic sphere vibrating radially without load is given in Ref. 1 and is shown in Fig. 4. C_o is the damped electrical capacitance, N is the electromechanical transformer ratio, C_M is the mechanical compliance, m_M is the equivalent mechanical mass, and R_M is the mechanical resistance due to losses in the material.

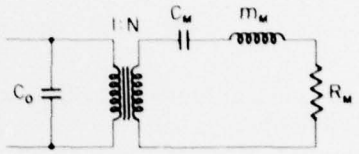

Fig. 4 — Lumped-constant equivalent circuit for a thin-walled ceramic sphere vibrating radially without load

Removing the transformer in the circuit of Fig. 4 and adding a voltage generator e_i to represent the transformed voltage due to the incident sound pressure, and a parallel resistance and inductance to represent the water load, the equivalent circuit shown in Fig. 5 is obtained. The reactive part of the radiation impedance is $M_R = S_o \rho_o a_o$ and the resistive part is $R_R = S_o \rho_o c_o$, where $S_o = 4\pi a_o{}^2$ with a_o the outer radius of the sphere, ρ_o is the density of water, and c_o is the speed of sound in water.

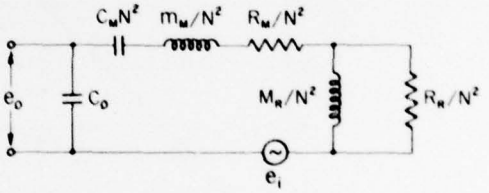

Fig. 5 — Equivalent circuit for a thin-walled ceramic spherical sensor with radiation load

Any difference in the acoustic phase between the loaded and the unloaded spheres is obviously caused by the radiation load impedance. The phase angle ϕ as a result of the radiation load is given by the ratio of the imaginary and real parts of the radiation impedance,

$$\phi = \tan^{-1} \frac{\omega M_R}{R_R} = \tan^{-1} \left(\frac{\omega a_o}{c_o} \right). \tag{9}$$

The wave number $k = 2\pi f/c_o$. Then,

$$\phi = \tan^{-1} ka_o. \tag{10}$$

Figure 6 is a graph of Eq. (10), which is the phase difference between a loaded and an unloaded hydrophone.

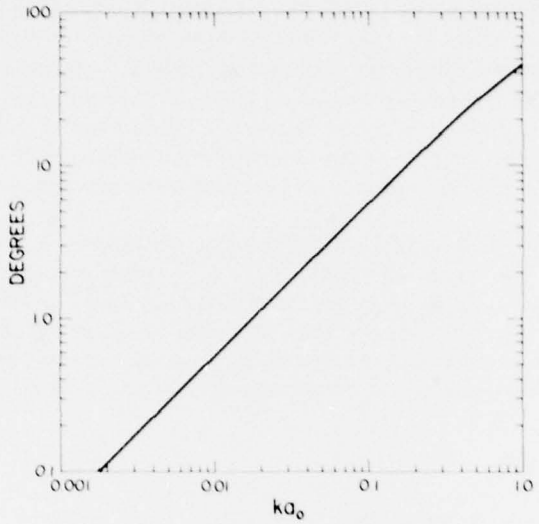

Fig. 6 — Phase difference in degrees between a loaded and an unloaded sphere as a function of ka_o

If we consider a typical spherical sensor element with radius a_o = 2.54 cm at a frequency of 100 Hz, then ka_o = 0.01 and $\phi = 0.6°$. Thus, for values where $ka_o \leq 0.01$, the difference in phase due to the radiation load on the sensor is negligible. As ka_o approaches 10^{-3}, the difference between the unloaded and loaded phases will be less than 0.1°.

This leads to several conclusions. First, within the constraint that $ka_o < 10^{-3}$, bench-top measurements of electrical phase via a calibration circuit will have the same value as those derived acoustically, because the electrical generator e_i of Fig. 5, representing the sound pressure, is equivalent to the calibrate input signal of a hydrophone with a conventional calibration circuit. This conclusion will be discussed further in the next section. Next, the phase calibration of a standard hydrophone can be verified in situ or can be accomplished anytime during a calibration as needed via the calibration circuit. An in-situ phase calibration of a loaded hydrophone can also be accomplished as a function of pressure, temperature, and frequency. Under these conditions a constant-phase standard hydrophone is not a requisite; only the ability to measure the phase is required. For a $ka_o > 0.001$, a bench measurement of phase can be accomplished and the results corrected by the value of $\tan^{-1} ka_o$ to give the equivalent loaded phase response.

Other physical effects of a hydrophone in a sound field are given in Appendices A and B.

ANALYSIS OF A CALIBRATION CIRCUIT FOR PHASE MEASUREMENTS

When the phase is determined via a calibration circuit, concern is not with the actual amplitude of the calibrator input or output signal as in a hydrophone coupling measurement, but only with the phase difference between the input signal and the hydrophone output. However, even though the measurement is straightforward in theory, some restrictions exist which determine the ultimate accuracy of the measurement.

Figure 7, from Ref. 2, depicts a hydrophone represented by a Thevenin generator with stray impedances shown in heavy dashed lines. The sensor is represented by the generator open-circuit voltage e_{oc} in series with generator impedance Z_g. The calibration resistor, typically 10 Ω, is small so that it does not attenuate the voltage e_{oc}, and therefore the calibration input voltage e_i is essentially an open-circuit voltage across the resistor; thus, e_i simulates e_{oc}. The voltage e_i is measured across a second external 10-Ω resistor shown as e_i'.

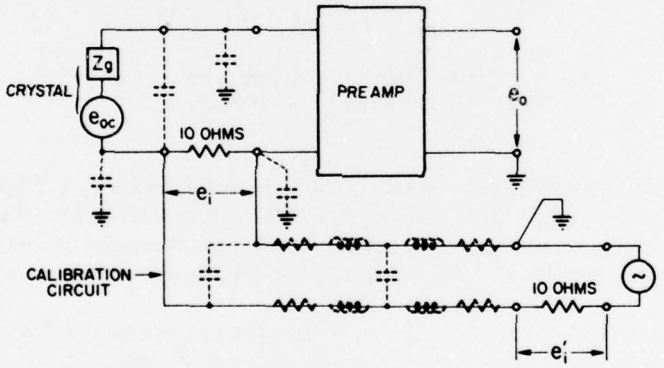

Fig. 7 — Hydrophone circuit as represented by a Thevenin generator and a preamplifier. Stray impedances are shown in heavy dashed lines.

For infrasonic and low audio frequencies, the calibration circuit can be represented as a lumped-parameter system as shown in Fig. 8. The hydrophone cable resistance is shown as R_c, the cable capacitance is C_c, and the calibration resistors are R_1 and R_2 respectively. The voltage e_i' is given by the product of R_1 and loop current i_1, and the resulting voltage at the internal calibration resistance is $e_i = i_2 R_2$. The ratio of i_2/i_1 is equal to the ratio of e_i/e_i'. Solving for i_2 and i_1 and the ratio i_2/i_1 gives

$$\frac{i_2}{i_1} = \frac{1}{1 + j\,\omega C_c R_T}, \tag{11}$$

where R_T is the total resistance. The phase angle of the voltage e_i and e_i' is then

$$\phi = \tan^{-1}\,(-\omega C_c R_T). \tag{12}$$

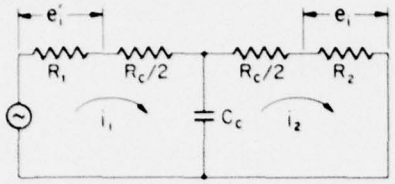

Fig. 8 — Lumped-parameter equivalent calibration circuit at infrasonic and low audio frequencies

For a typical case the cable resistance for a 30-m cable is about 2 Ω and the cable capacitance is 44.3×10^{-10} F. With 10-Ω calibration resistors the resulting phase angle ϕ at 100 Hz would be 0.0017°.

For phase measurement purposes at low frequencies, e_i' will be of the same phase as e_i if the reactive part of the cable impedance is several orders of magnitude greater than the calibration resistors. Under the same frequency and impedance restrictions, the cable can be several hundred meters long. This analysis does not imply an accurate determination of the magnitude of e_i' due to the real part of the cable impedance but merely an accurate determination of phase.

CHARGE EFFECTS ON LONG TIME-CONSTANT HYDROPHONES

The RC time constant (TC) is about 16 s for a hydrophone with a constant phase down to 1 Hz (f_o = 0.01 Hz). The long TC makes the preamplifier very susceptible to charge voltages generated by the sensor due to slight changes in hydrostatic pressure or temperature. The charge biases off the input transistor of the preamplifier because it cannot be rapidly dissipated. In small-volume, high-pressure systems, hydrostatic and thermodynamic equilibrium is difficult, if not impossible, to realize. Therefore, the hydrophone can be inoperative for several minutes after a pressure or temperature change, and can remain inoperative if slight changes persist.

The preamplifier input voltage can be represented as shown in Fig. 9 if the sensor-element output voltage is generated by changes in hydrostatic pressure or temperature. The sensor-output charge voltage q as a function of time t is $e_s(t)$; C_s is the free capacitance of the sensor; R is the total shunt resistance across C_s; and $e_i(t)$ is the voltage input at the preamplifier FET. The equation for $e_s(t)$ in this circuit is

$$e_s(t) = R_i(t) + \frac{1}{C}\int i(t)dt, \quad t \geq 0. \tag{13}$$

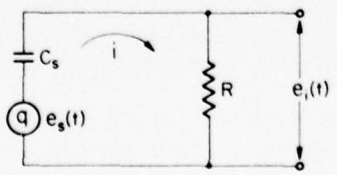

Fig. 9 — Simplified equivalent circuit for hydrophone input charge voltages

If $e_s(t)$ is defined as a linear function of time, then a solution of Eq. (13) for $e_i(t)$ is

$$R_i(t) = e_i(t) = ARC(1-e^{-\delta t}),\ t > 0, \tag{14}$$

where $\delta = 1/RC$ (derivation of this equation is given in Appendix C) and A is a constant linear function in the time domain. Thus $A \equiv MdP/dt + \theta d\theta/dt$ where the time differentials are constants. Then $M \equiv$ piezoelectric pressure sensitivity of the acoustic sensor in volts per unit pressure, $dP/dt \equiv$ constant rate of change of pressure with time, $\theta \equiv$ pyroelectric sensitivity of the acoustic sensor in $V/^{\circ}C$, and $d\theta/dt \equiv$ constant rate of change of temperature with time:

$$\Rightarrow e_i(t) = (MdP/dt + \theta d\theta/dt)RC(1 - e^{-\delta t}),\ t > 0. \tag{15}$$

If Eq. (15) is normalized, then the classical resistor voltage transient curve for an RC circuit as shown in Fig. 10 is obtained, where

$$E_R = \left(1 - e^{-\delta t}\right). \tag{16}$$

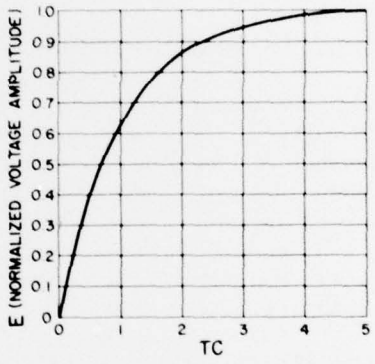

Fig. 10 — Normalized charge voltage at the hydrophone preamplifier input for all general hydrophone cases

Figure 10 now represents all general hydrophone cases. For a specific case, $e_i(t)$ as a function of temperature and hydrostatic pressure is simply the product of the abscissa value and $(MdP/dt + \theta d\theta/dt)RC$.

Now consider a hydrophone with a spherical sensor of Navy Type I material [3] with an outside radius of 1.27 cm and an inside radius of 0.95 cm. The nominal open-circuit sensitivity is about −200 dB re 1 $V/\mu Pa$, and the nominal capacitance is 5.5×10^{-9} F. The physical dimensions give a $ka_o < 0.005$ at frequencies below 100 Hz. With a preamplifier input impedance of $2.9 \times 10^9\ \Omega$, the time constant $RC = 16$ s. The hydrophone thus meets the design criterion for a constant phase response at frequencies down to 1 Hz.

Now, using Eq. (15), the charge voltage $e_i(t)$ that can exist at the input of the hydrophone preamplifier as a function of temperature and hydrostatic pressure is evaluated.

First, the absolute value of the charge voltage at a constant temperature is given as a function of time and pressure:

$$\left|e_i(t)\right|_\theta = (MdP/dt)RC\,(1 - e^{-\delta t}), \tag{17}$$

where RC = 16 s, M = -200 dB re 1 $V/\mu Pa$ or 10^{-4} V/Pa, and dP/dt is a linear change of hydrostatic pressure with time. Figure 11 shows the charge voltage generated for three specific dP/dt rates.

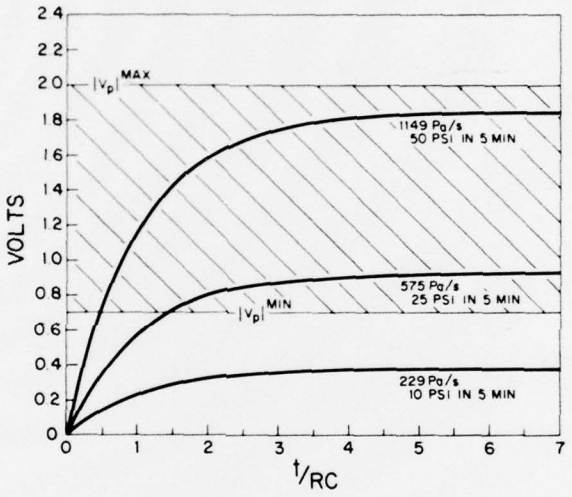

Fig. 11 — Absolute value of the charge voltage at the preamplifier input at a constant temperature as a function of three dP/dt rates for a specific hydrophone

Also shown in Fig. 11 is the range of the absolute value of the pinch-off voltage V_p for an FET (2N4867) commonly used as the input stage in hydrophone preamplifiers. When the voltage between the gate and source (V_{GS}) of the transistor is such that $|V_{GS}| \geqslant |V_p|$, then the channel current of the FET is cut off. For a specific transistor, V_p will be some specific value within the V_p range. If V_p is at the lower end of the voltage range and the dP/dt rate is 575 Pa/s (25 psi in 5 min), after 24 s the charge voltage will approach V_p. When this happens, in the lexicon of the art, "the hydrophone is blocked," and measurements must wait until it decides to "wake up."

For a Type I material the pyroelectric effect below 80°C is 0.026×10^{-6} coul/cm^2°C. For the hydrophone under consideration, the pyroelectric sensitivity will be about 72 V/°C (see Appendix D for computation of the pyroelectric sensitivity). The absolute value of

the charge voltage at a constant pressure as a function of time and temperature from Eq. (15) is

$$\left|e_i(t)\right|_p = (\theta d\theta/dt)RC\,(1 - e^{-\delta t}), \tag{18}$$

where RC = 16 s, θ = 72 $V/°C$, and $d\theta/dt$ is a linear change of temperature with time. Figure 12 shows $|e_i(t)|_p$ for three specific $d\theta/dt$ rates. A very small temperature change such as 0.001°C/s (0.3°C in 5 min) develops sufficient voltage to block an average FET.

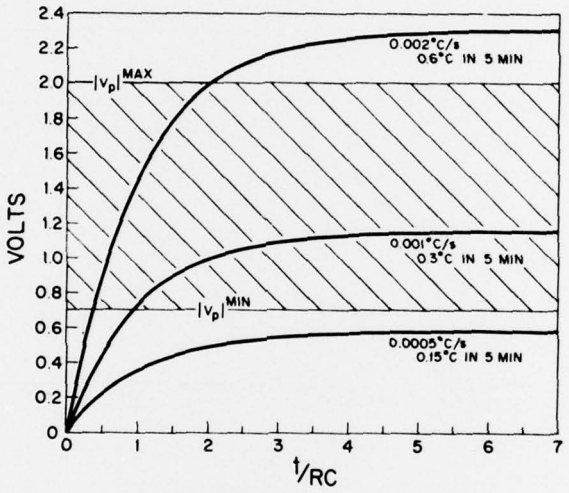

Fig. 12 — Absolute value of the charge voltage at the preamplifier input at a constant pressure as a function of three $d\theta/dt$ rates for a specific hydrophone

Figures 11 and 12 present $e_i(t)$ in terms of absolute values because the charge polarity will depend on whether the pressure or temperature is increasing or decreasing and upon the polarization of the crystal-preamplifier connections. Also, the presented analysis is idealized because in reality dP/dt and $d\theta/db$ are not linear, but exponential functions. However, the analysis does demonstrate that the hydrostatic pressure and temperature changes will generate a charge voltage at the preamplifier input which can be detrimental if the TC is large. The effect of the temperature change could add to or subtract from the effect of the pressure change, depending upon whether the temperature increases or decreases. Either condition could be experienced, but the worst case should be anticipated; that is, the effects add.

PIEZOELECTRIC MATERIAL CONSIDERATIONS

If a hydrophone is to have a constant phase response down to 1 Hz with sensor restrictions of $ka_o \leq 0.005$ at $f \leq 100$ Hz and if good acoustic sensitivity and a hydrostatic pressure capability of 70 MPa are added to the specifications, then certain material limitations exist that will cause some design compromises. In the previous example, the TC for the hydrophone would be 16 s. This gives the restriction that either the sensor capacitance has to be large or the preamplifier input impedance very high. Setting the preamplifier input impedance in a partial range of 10^9 to 10^{10} Ω puts the sensor capacitance in the range of 1.6×10^{-9} to 1.6×10^{-8} F.

If the sensor were constructed of lithium sulfate or lead metaniobate, a large number of crystals would be needed to get the desired capacitance, and the desired ka_o would be exceeded. However, both materials would be suitable for high-pressure applications, with lithium sulfate being the preferred material but having the lowest dielectric constant (10.3).

Examination of the lead zirconate titanate materials would lead to the exclusion of Navy Type II, because its dielectric constant and sensitivity vary with hydrostatic pressure [4]. Depolarization may occur in some configurations at pressures to 70 MPa. In most cases the Type II material is the most desirable of the Navy types because it has the highest dielectric constant. It is suitable for applications from about 10 to 30 MPa with the exact pressure limit depending on the dimension and configuration of the sensor, but it is not appropriate in this case.

Type I and Type III materials are the most stress resistant of the Navy materials. Type I material has a moderately high dielectric constant and has been used with good results in high-pressure applications. The Type III material is a high-stress ceramic with the lowest dielectric constant compared to the Type I and Type II materials, but its dielectric constant is four times higher than lead metaniobate and two orders of magnitude higher than lithium sulfate. Even though the Type I and Type III materials are more stress resistant, their sensitivities and dielectric constants still vary as a function of hydrostatic pressure [4].

Two-dimensional stress data on some radially polarized capped cylinders of Type I and Type III materials with different diameter-to-wall thickness ratios (d/t) are given in Table 1. In each case, $ka_o < 0.01$ at 100 Hz. The table indicates the material type and the d/t ratio; Δk_3 is the percentage of change in the relative dielectric constant, and ΔM_o represents the change in acoustic sensitivity (dB re 1 $V/\mu Pa$) in the flat portion of the response. In this discussion, more concern is placed on the dielectric constant than on sensitivity because of its direct effect on the sensor capacitance and phase. The table shows that the dielectric constant has decreased by 57% in two of the sensors at 70 MPa. The decrease in dielectric constant represents an increase in f_o in excess of one octave. Subsequently, the phase has shifted over 18° from what it was at lower pressures.

Several years ago, the USRD began using spherical sensors at pressures up to 70 MPa [5] with the emphasis being on sensitivity stability. A sphere with a d/t ratio of 8 made from a Type I material experiences a reduction in sensitivity of 1.5 dB [6], but the

Table 1 — Two-Dimensional Stress Data on Some Radially Polarized Capped Cylinders of Type I and Type III Materials with Different Diameter-to-Wall Thickness Ratios*

Navy Type	d/t Ratio	35 *MPa*		70 *MPa*	
		Δk_3(%)	Δ *Mo* (dB)	Δk_3(%)	Δ *Mo* (dB)
Type I	6.3	-10.6	-1.0	-38	-3.0
Type III	6.3	0	-0.8	-57	-2.5
Type I	9.7	0	-1.0	0	-3.2
Type III	9.7	-27	-1.0	-57	-3.2

*Names of material manufacturers are available upon request.

dielectric constant behaves much like that of the cylindrical configuration with a 15—18% decrease at 35 *MPa* and a 35—40% decrease at 70 *MPa*.

In addition to hydrostatic pressure effects, temperature also has a significant effect on the dielectric constant of lead zirconate titanate ceramics. Manufacturers' data indicate that in the temperature range from 0 to 40°C the dielectric constant of Type I material will increase from 5 to 15%, that of Type II will increase 15 to 25%, and that of Type III will increase from 5 to 10%. Obviously, the effect of temperature on the dielectric constant has a direct effect on phase stability.

These material considerations lead to the following conclusions. First, a phase reference standard using a lead zirconate titanate ceramic sensor should be phase calibrated as a function of temperature, hydrostatic pressure, and frequency—especially in the frequency range two decades above f_o. This can be accomplished in situ as required within the constraints previously discussed. Second, a reference hydrophone whose phase is not constant at frequencies down to 1 Hz but is stable with temperature and hydrostatic pressure is preferable to one whose phase is constant with frequency but varies with temperature and hydrostatic pressure.

Lithium sulfate is the preferred sensor material for a hydrophone whose phase is virtually independent of hydrostatic pressure and temperature. USRD measurements in a high-pressure reciprocity coupler have shown that the dielectric constant changes about 0.0175%/*MPa* at hydrostatic pressures to 110 *MPa*. In the temperature range from 0 to 40°C, the dielectric constant changes less than 2% (0.047%/°C) [7]. The volume of material required may exceed desirable ka_o limitations, and the capacitance would be too small to have f_o at 0.01 Hz. But these compromises are reasonable for the best phase stability as a function of hydrostatic pressure and temperatures.

CONCLUSIONS

For a hydrophone to have a constant phase response down to 1 Hz, f_o must be set at 0.01 Hz. This gives a TC of 16 s, which makes the hydrophone highly susceptible to charge effects from temperature and pressure changes.

Bench-top measurements of phase via a calibration circuit will have the same value as those derived acoustically if the size of the sensor is such that $ka_o < 10^{-3}$ at $f \leq 100$ Hz. At infrasonic and low audio frequencies, phase measurements can be made in situ (i.e., the standard can be phase calibrated) with a calibrate circuit and the ka_o restriction. No error will result if the reactive part of the cable impedance is several orders of magnitude greater than the calibration resistors.

The dielectric constant of lead zirconate titanate changes as a function of temperature and hydrostatic pressure, which can cause a significant change in the phase response of a hydrophone.

Lithium sulfate is the preferred sensor material for a phase-stable reference standard even though its dielectric constant is two orders of magnitude less than the ceramics.

ACKNOWLEDGMENT

The authors wish to thank George D. Hugus of the USRD for his help in the theoretical analysis of the charge effects in long TC hydrophones.

REFERENCES

1. W.P. Mason (ed.), *Physical Acoustics*, Vol. I, Part A, Academic Press, New York, 1964, p. 223.
2. R.J. Bobber, *Underwater Electroacoustic Measurements*, Naval Research Laboratory, Government Printing Office, Washington, D.C., 1970, p. 137.
3. MIL-STD-1376 (SHIPS), "Piezoelectric Ceramic for Sonar Transducers," Dec. 21, 1970, FSC 584.
4. S.W. Meeks and R.W. Timme, "Effects of One-Dimensional Stress on Piezoelectric Ceramics," J. Appl. Phys. 46, 4334, Oct. 1975.
5. L.E. Ivey, "High-Pressure Piezoelectric Ceramic Hydrophone for Infrasonic and Audio Frequencies USRD Type H48," NRL Rept. 7260, Mar. 15, 1971.
6. T.A. Henriquez, "Calibration at High Pressure of Piezoelectric Elements for Deep-Submergence Hydrophones," J. Acous. Soc. Amer., 46, No. 5 (Part 2): 1251, Nov. 1969.
7. W.P. Mason, *Piezoelectric Crystals and Their Application to Ultrasonics*, D. Van Nostrand Co. Inc., New York, 1950, p. 229.

Appendix A

THE EFFECT OF RIGGING INACCURACIES ON COMPARATIVE PHASE MEASUREMENTS

In general, most requirements for electroacoustic phase measurements are for low frequencies (below 100 Hz). For accurate determination of the phase response of an unknown hydrophone by comparison with a standard hydrophone, the acoustic centers of both hydrophones must be in the same plane normal to the direction of the acoustic plane wave. If the acoustic centers are not *perfectly* aligned, an error in phase results due to the acoustic delay caused by the relative positions of the standard and the unknown hydrophones. If the two acoustic centers are displaced a distance Δd in the direction of the plane wave, then the resulting relative phase measurement will be in error by

$$\Delta\phi \frac{2nf}{c} \Delta d, \tag{A1}$$

where f is the frequency of the acoustic wave and c is the propagation speed of the acoustic wave. From Eq. (A1), the error in phase due to a 1-cm error in rigging at 100 Hz is

$$\Delta\phi = \frac{2nf}{c} \Delta d = \frac{360f}{c} \Delta d = \frac{360(100)}{1500}(0.01)$$

$$\Delta\phi = 0.24 \text{ degrees.}$$

For a maximum allowable error in a phase measurement of 0.1° due to rigging, the maximum rigging error is given as a function of frequency by Fig. A1. Multiplying the ordinate of Fig. A1 translates the graph to a maximum allowable error of 1.0°.

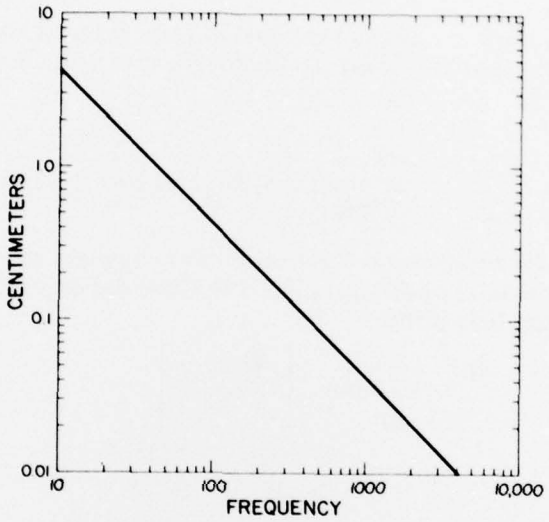

Fig. A1 — Rigging accuracy between a standard and an unknown hydrophone for a phase resolution 0.1°

Appendix B

PHASE RESPONSE OF A SPHERICAL HYDROPHONE ELEMENT DUE TO DIFFRACTION

For a spherical hydrophone element exposed to plane acoustic waves, the average pressure over the spherical surface relative to the free-field pressure in the absence of the sphere is*

$$\frac{P_{AV}}{P_{ff}} = \frac{(ka_o)^2}{1 + (ka_o)^2}\left[n_i(ka_o) + i\,j_i(ka_o)\right], \tag{B1}$$

where a is the radius of the sphere, k is the acoustic wave number, and n_i and j_i are spherical Neumann and Bessel functions of the first kind. The phase response of the hydrophone due to the diffracted pressure field is then

$$\phi = \tan^{-1}\left[\frac{j_1(ka_o)}{n_1(ka_o)}\right], \tag{B2}$$

$$j_1(ka_o) = \frac{sin(ka_o)}{(ka_o)^2} - \frac{cos(ka_o)}{(ka_o)}, \tag{B3}$$

and

$$n_1(ka_o) = -\frac{sin(ka_o)}{(ka_o)} - \frac{cos(ka_o)}{(ka_o)^2}. \tag{B4}$$

Then

$$\phi = \tan^{-1}\left[-\frac{sin(ka_o) - (ka_o)cos(ka_o)}{(ka_o)sin(ka_o) + cos(ka_o)}\right]. \tag{B5}$$

Figure B1 is a plot of the phase angle between the free-field pressure and the response of the spherical element due to diffraction.

*T.A. Henriquez, "Diffraction Constants of Acoustic Transducers," J. Acous. Soc. Am. 36, 267-269 (1964).

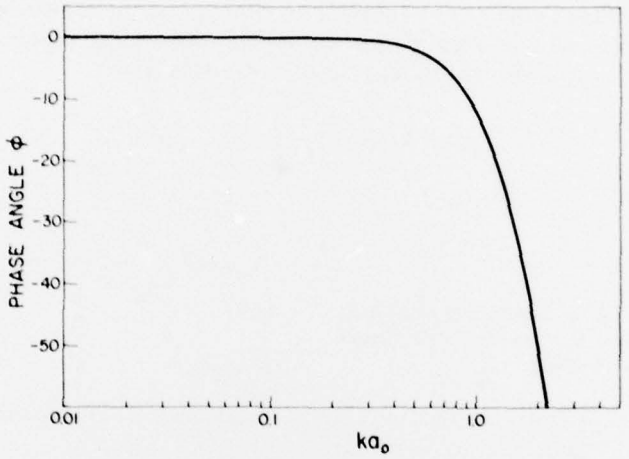

Fig. B1 — Phase angle between the free-field pressure and the response of the spherical element due to diffraction

Appendix C

DERIVATION OF THE CHARGE VOLTAGE EQUATION

If the sensor-element output voltage is generated by changes in temperature or hydrostatic pressure, the preamplifier input voltage generated is as shown in Fig. C1 where $e_s(t)$ is the sensor output voltage as a function of time t, C is the sensor capacitance, R is the total shunt resistance across the sensor, and $e_i(t)$ is the voltage at the input of the preamplifier. The equation for the current in this circuit loop is

$$e_s(t) = i(t)R + \frac{1}{C}\int i(t)dt, \quad t \geqslant 0. \tag{C1}$$

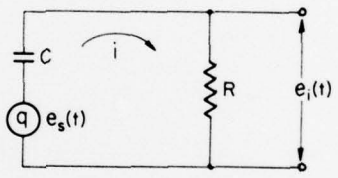

Fig. C1 — Simplified equivalent circuit for hydrophone input charge voltages.

If $e_s(t)$ is a linear function of time, then

$$e_s(t) = At. \tag{C2}$$

Substituting Eq. (C2) into Eq. (C1) results in

$$At = iR + \frac{1}{C}\int i\,dt. \tag{C3}$$

Taking the LaPlace transform gives

$$\frac{A}{s^2} = I(s)\,R + \frac{1}{C}\left[\frac{I(s)}{s}\right]. \tag{C4}$$

In solving for $I(s)$ and simplifying, we obtain

$$I(s) = \frac{A}{R}\left[\frac{1}{s(s + 1/RC)}\right]. \tag{C5}$$

Expanding Eq. (C5) gives

$$I(s) = AC\left[\frac{1}{s} - \frac{1}{s + 1/RC}\right]. \tag{C6}$$

Take the inverse transform of Eq. (C6):

$$i(t) = AC\left(u(t) - e^{-t/RC}\right). \tag{C7}$$

Let $\delta = \dfrac{1}{RC}$. Then the voltage $e_i(t)$ from Eq. (C7) is

$$e_i(t) = i(t)R = ARC\left(u(t) - e^{-\delta t}\right), \quad t \geq 0. \tag{C8}$$

This becomes, in the time domain,

$$e_i(t) = -ARC, \quad t = 0; \tag{C9}$$

$$e_i(t) = ARC\left(1 - e^{-\delta t}\right), \quad t > 0. \tag{C10}$$

If $A = MdP/dt + \theta d\theta/dt$ where dP/dt and $d\theta/dt$ are independent constant linear functions of time, then

$$e_i(t) = (MdP/dt + \theta d\theta/dt)RC\left(1 - e^{-\delta t}\right), \quad t > 0. \tag{C11}$$

If $d\theta/dt = 0$, then

$$\left|e_i(t)\right|_\theta = (MdP/dt)RC\left(1 - e^{-\delta t}\right), \quad t > 0. \tag{C12}$$

Conversely if $dP/dt = 0$, then

$$\left|e_i(t)\right|_p = (\theta d\theta/dt)RC\left(1 - e^{-\delta t}\right), \quad t > 0. \tag{C13}$$

Appendix D

PYROELECTRIC SENSITIVITY OF A SPHERE

The pyroelectric sensitivity of a ceramic sensor is computed from the fundamental relationship of voltage, charge, and capacitance where

$$E = \frac{Q}{C} \tag{D1}$$

and $Q \equiv$ charge per unit area °C. The pyroelectric effect $(\partial P/\partial\theta)_T$ is given in manufacturers' data in units of charge (C) per unit area °C.* For Type 1 material, $Q = 0.026 \times 10^{-2}$ C/m^2°C. Since 1 farad = 1 coulomb/volt, then Eq. (D1) gives the pyroelectric sensitivity in volts per unit area °C.

Now consider a spherical sensor of Type I material of outside radius $b = 1.27 \times 10^{-2}$m and inside radius $a = 9.5 \times 10^{-3}$m. The capacitance is given by

$$C = 4\pi\epsilon \frac{ab}{b-a}, \tag{D2}$$

where $\epsilon = K_{33}^T \epsilon_0$, with K_{33}^T *being the free relative* dielectric constant of the material and $\epsilon_0 = 8.85 \times 10^{-12} F/m$ the permittivity of free space. $K_{33}^T = 1300$ for Type I material, which gives a capacitance of 5.5×10^{-9} F using Eq. (D2).

The effective electrode area of the sphere is given by the fundamental equation of capacitance

$$C = \frac{A\epsilon}{d}, \tag{D3}$$

where A is the area of the plates and d is the distance between the plates. For the sphere, $d = b - a$. Substituting $b - a$ in Eq. (D3) for d and Eq. (D2) in Eq. (D3) for C, we obtain

$$4\pi\epsilon \left(\frac{ab}{b-a}\right) = \frac{A\epsilon}{(b-a)}. \tag{D4}$$

Solving for A gives

$$A = 4\pi ab, \tag{D5}$$

the effective electrode area. For the considered sphere, Eq. (D5) gives 1.516×10^{-3}m^2.

*"Piezoelectric Technology Data for Designers," Clevite Corp., Bedford, Ohio, 1965, p. 36.

Using Eqs. (D1) and (D5), the pyroelectric sensitivity can now be expressed in $V/^{\circ}C$ as

$$E = \frac{Q}{C}(A) = \frac{0.026 \times 10^{-2}}{5.5 \times 10^{-9}}(1.516 \times 10^{-3}) = 71.7\ V/^{\circ}C. \qquad \text{(D6)}$$